Positive and Negative Roles of Homologous Recombination in the Maintenance of Genome Stability in *Saccharomyces cerevisiae*

Jumpei Yoshida,* Keiko Umezu*,†,[1] and Hisaji Maki*

**Department of Molecular Biology, Graduate School of Biological Sciences, Nara Institute of Science and Technology, Ikoma, Nara 630-0192, Japan and* †*PREST, Japan Science and Technology Corporation, Kawaguchi, Saitama 332-0012, Japan*

Manuscript received October 17, 2002
Accepted for publication January 8, 2003

ABSTRACT

In previous studies of the loss of heterozygosity (LOH), we analyzed a hemizygous *URA3* marker on chromosome III in *S. cerevisiae* and showed that homologous recombination is involved in processes that lead to LOH in multiple ways, including allelic recombination, chromosome size alterations, and chromosome loss. To investigate the role of homologous recombination more precisely, we examined LOH events in *rad50*Δ, *rad51*Δ, *rad52*Δ, *rad50*Δ *rad52*Δ, and *rad51*Δ *rad52*Δ mutants. As compared to Rad$^+$ cells, the frequency of LOH was significantly increased in all mutants, and most events were chromosome loss. Other LOH events were differentially affected in each mutant: the frequencies of all types of recombination were decreased in *rad52* mutants and enhanced in *rad50* mutants. The *rad51* mutation increased the frequency of ectopic but not allelic recombination. Both the *rad52* and *rad51* mutations increased the frequency of intragenic point mutations ~25-fold, suggesting that alternative mutagenic pathways partially substitute for homologous recombination. Overall, these results indicate that all of the genes are required for chromosome maintenance and that they most likely function in homologous recombination between sister chromatids. In contrast, other recombination pathways can occur at a substantial level even in the absence of one of the genes and contribute to generating various chromosome rearrangements.

LOSS of heterozygosity (LOH) is an important process that causes gene inactivation in diploid cells. For cells with a pair of functional alleles, two genetic events are usually required to cause phenotypic changes, each involving an alteration of an allele. If one of the alleles carries a recessive mutation, such as a point mutation, a second event that creates LOH could be any genetic alteration that inactivates the remaining allele. Thus, genetic alterations leading to phenotypic changes are more complex in diploid cells than in haploid cells. In addition, accumulating evidence indicates that various processes required for the maintenance of chromosomal integrity in yeast are sensitive to ploidy or to the status of the mating-type locus (Heude and Fabre 1993; Klein 1997; Astrom *et al.* 1999; Bennett *et al.* 2001), which has different implications for genetic alterations in haploid and diploid cells.

In previous studies, we analyzed spontaneous LOH events in *Saccharomyces cerevisiae* diploids that lead to functional inactivation of a hemizygous *URA3* marker inserted at the center of the right arm of chromosome III under vegetative growth conditions (Hiraoka *et al.* 2000; Umezu *et al.* 2002). In this assay, the frequency of LOH events is $1–2 \times 10^{-4}$, three orders of magnitude greater than the frequency of spontaneous mutation affecting the *URA3* marker in haploid cells. An analysis of chromosome structure showed that the major classes of LOH events were chromosome loss, allelic recombination, and ectopic recombination leading to aberrant-sized chromosomes. Homologous recombination contributed to at least half of these alterations. Allelic recombination, which includes both crossing over and local gene conversion, was responsible for 30–35% of the LOH events. Chromosome III derivatives of aberrant size were readily detected in ~8% of the LOH clones. To identify the breakpoints in these aberrant chromosomes, we established a PCR-based method to quantify the ploidy of a series of loci along chromosome III (Umezu *et al.* 2002). Almost all of the breakpoints in wild-type cells were within repetitive sequences: the retrotransposon Ty1 was involved in various translocation and unequal crossing-over events, and the *MAT-HMR* loci were exclusively implicated in intrachromosomal deletions. Thus, the chromosome rearrangements identified in the assay arose mainly through homologous recombination between allelic or ectopic sites throughout the yeast genome. In addition, homologous recombination is implicated in chromosome loss. Chromosome loss contributed to ~60% of all LOH events, and, in at least 4% of the cases, the remaining chromosome was an interchromosomal recombinant. The frequencies of the events observed indicate that at least some recombination is nonconservative and contributes to chromosome loss (Hiraoka *et al.* 2000). Thus, homol-

[1]*Corresponding author:* Department of Molecular Biology, Graduate School of Biological Sciences, Nara Institute of Science and Technology, Takayama 8916-5, Ikoma, Nara 630-0192, Japan.
E-mail: umezu@bs.aist-nara.ac.jp

ogous recombination plays significant roles in cellular processes leading to LOH in multiple ways.

Mitotic homologous recombination in *S. cerevisiae* is mediated by multiple pathways that require distinct subsets of genes (reviewed in Paques and Haber 1999 and Sung *et al.* 2000). These genes belong to the *RAD52* epistasis group and were primarily identified as mutations conferring sensitivity to X rays; these and more recently identified genes can be classed into four subgroups on the basis of their roles in mitotic recombination. First, the *RAD52* gene is essential for virtually all forms of homologous recombination, including gene conversion, single-strand annealing (SSA), and break-induced replication (BIR). The Rad52 protein (Rad52p) promotes Rad51-mediated strand exchange and DNA annealing. Recently, human Rad52p itself has also been shown to mediate D-loop formation (Kagawa *et al.* 2001). Second, the *RAD51* subgroup (*RAD51*, *RAD54*, *RAD55*, and *RAD57*) is involved in gene conversion and certain types of BIR, but not in SSA initiated by a double-strand break (DSB). These properties appear to reflect the biochemical activities of their gene products. Rad51p, a homolog of bacterial RecA, plays a key role in homologous DNA pairing and strand exchange. Rad55p and Rad57p form a complex that stimulates Rad51-mediated strand exchange at the initial step. Rad54p is a member of the Swi2/Snf2 family and promotes homologous pairing by Rad51p by an undetermined mechanism. Third, *RAD52*-dependent and *RAD51*-independent recombination pathways require *RAD59* and *TID1/RDH54* (Bai and Symington 1996; Signon *et al.* 2001). Rad59p has some homology to Rad52p, while *TID1/RDH54* encodes a homolog of Rad54p. And finally, *RAD50*, *MRE11*, and *XRS2* define another group of genes required for homologous recombination and for nonhomologous end joining (NHEJ) and the maintenance of telomere length. Their products form a complex (MRX) that is involved in the processing of DSB ends and that has also been implicated as a sensor for a DNA damage checkpoint (Grenon *et al.* 2001; Usui *et al.* 2001).

In this study, to investigate the roles of homologous recombination in LOH more precisely, we examined LOH events in *rad50*Δ, *rad51*Δ, *rad52*Δ, *rad50*Δ *rad52*Δ, and *rad51*Δ *rad52*Δ homozygous diploids. In all mutant strains, the frequency of chromosome loss was significantly increased compared to Rad$^+$ cells, indicating that all of these genes are required for proper chromosome maintenance. In addition, the frequency of point mutations was significantly elevated in both *rad52* and *rad51* mutants, presumably through alternative mutagenic pathways that substitute for homologous recombination. On the other hand, each mutation had different effects on individual types of chromosome rearrangements and the majority of these events were *RAD52* dependent, revealing that multiple recombination pathways are involved in processes leading to genome instability. Thus, homologous recombination plays both positive and negative roles in the maintenance of genome stability.

MATERIALS AND METHODS

Media: Media for yeast strains, including complex glucose (YPD), synthetic complete (SC), and various drop-out media, were prepared as previously described (Rose *et al.* 1990). For YPAD medium, adenine sulfate was added to YPD to a final concentration of 0.004%. Uracil was added to YPAD to 20 μg/ml where indicated. 5-Fluoro-orotic acid (5-FOA) plates were prepared as described (Rose *et al.* 1990) and depleted for leucine and/or adenine sulfate where indicated. Methyl methanesulfonate (MMS) was added to YPD to a final concentration of 0.01% when required. *Escherichia coli* cells were grown in LB medium (Sambrook *et al.* 1989) supplemented with 100 μg/ml ampicillin when required.

Genetic and nucleic acid techniques: Standard genetic manipulations for yeast were followed (Rose *et al.* 1990). General DNA manipulations were performed as described (Sambrook and Russell 2001). Yeast genomic DNA was isolated using the GenTLE yeast kit (Takara, Tokyo). The QIAquick gel extraction kit (QIAGEN, Hilden, Germany) was used for extracting DNA from agarose plugs. PCR products used as probes for Southern hybridization were purified with the QIAquick PCR purification kit (QIAGEN).

Plasmids: pMO317, an *ARS-CEN-LYS2* plasmid carrying the *RAD52* gene, was constructed by subcloning the *Bsa*I-*Eag*I *RAD52*-containing fragment of ScRAD52pRS316 into the corresponding sites of the vector pRS317. ScRAD52pRS316 carries the 3.2-kb *Eco*RI-*Sal*I *RAD52*-containing fragment from YpSL1 (Adzuma *et al.* 1984) in the *Eco*RI-*Xho*I cloning site of pRS316, kindly provided by Dr. A. Shinohara of Osaka University. To construct deletion strains, the following fragments containing the *hisG-URA3-hisG* disruption construct were used: the 6.4-kb *Eco*RI-*Bgl*II fragment of pNKY83 (Alani *et al.* 1989) for *RAD50*, the 6.3-kb *Bam*HI fragment of pΔRAD51 (Shinohara *et al.* 1992) for *RAD51*, and the 6.4-kb *Eco*RI-*Sal*I fragment of pHT19 (Ogawa *et al.* 1993) for *RAD52*. pHT19 is a pBR322 derivative that contains the *hisG-URA3-hisG* fragment between the 1.2-kb *Eco*RI-*Cla*I fragment and the 1.4-kb *Bam*HI-*Sal*I fragment, both of which are derived from YpSL1. These disruption plasmids were a generous gift from Dr. T. Ogawa (National Institute of Genetics). pU6H2MYC, which contains the 6His-2MYC-loxP-*kan*MX-loxP module (De Antoni and Gallwitz 2000), was kindly provided by Dr. K. Shirahige of Genomic Science Center, RIKEN (Yokohama, Japan).

Strains: All yeast strains used in this study are derivatives of YKU23 (*MAT*α *lys2*Δ*202 leu2*Δ*1 ura3-52 his3*Δ*200 ade2*Δ::*hisG*) and YKU34 (*MAT***a** *lys2*Δ*202 ura3-52 trp1*Δ*63 ade2*Δ::*hisG III*-205::*URA3 III*-314::*ADE2*) with the S288c background (Hiraoka *et al.* 2000) and are listed in Table 1. *III*-205::*URA3* signifies that the *URA3* fragment was inserted at a locus 205 kb from the left end of chromosome III. Similarly, *III*-314::*ADE2* denotes that the *ADE2* fragment was inserted at 314 kb. Nucleotide coordinates are as given in the Saccharomyces Genome Database (SGD; http://genome-www.stanford.edu/Saccharomyces/). Haploid strains defective for the *RAD* genes were constructed by transforming YKU23 or YIY1 with *hisG-URA3-hisG* disruption construct fragments (described in the *Plasmids* section), followed by selection of clones that had lost the *URA3* marker between the repetitive *hisG* sequences (Alani *et al.* 1987). The *rad52*, *rad51*, and *rad50* derivatives of YKU23 were designated as YMO2, YMO6, and YMO4, and YIY1 derivatives were designated as YMO1, YMO5, and YMO3, respectively. Gene disruption was verified by PCR of the locus and by examination of MMS sensitivity on YPD-MMS plates. Introduc-

TABLE 1

Genotypes of the yeast strains

Strain	Genotype	Origin
	Haploids	
YKU1	*MAT***a** *lys2Δ202 leu2Δ1 ura3-52 trp1Δ63*	Hiraoka *et al.* (2000)
YKU23	*MAT*α *lys2Δ202 leu2Δ1 ura3-52 his3Δ200 ade2*Δ::*hisG*	Hiraoka *et al.* (2000)
YKU34	YKU1 except *LEU2 ade2*Δ::*hisG III*-205::*URA3*[a] *III*-314::*ADE2*[b]	Hiraoka *et al.* (2000)
YIY1	YKU1 except *LEU2 ade2*Δ::*hisG III*-314::*ADE2*	This study
YMO2	YKU23 except *rad52*Δ::*hisG*	This study
YMO4	YKU23 except *rad50*Δ::*hisG*	This study
YMO6	YKU23 except *rad51*Δ::*hisG*	This study
YMO7	YKU34 except *rad50*Δ::*hisG*	This study
YMO8	YKU34 except *rad51*Δ::*hisG*	This study
YMO9	YKU34 except *rad52*Δ::*hisG*	This study
YMO50	YKU23 except *rad52*Δ::*hisG rad51*Δ::*kan*MX[c]	This study
YMO51	YKU34 except *rad52*Δ::*hisG rad51*Δ::*kan*MX	This study
YMO52	YKU23 except *rad52*Δ::*hisG rad50*Δ::*kan*MX	This study
YMO53	YKU34 except *rad52*Δ::*hisG rad50*Δ::*kan*MX	This study
	Diploids	
RD301	*MAT***a**/*MAT*α *lys2Δ202/lys2Δ202 LEU2/leu2Δ1 ura3-52/ura3-52 trp1Δ63/TRP1 HIS3/his3Δ200 ade2*Δ::*hisG/ade2*Δ::*hisG III*-205::*URA3/III*-205 *III*-314::*ADE2/III*-314	YKU23 × YKU34
RD304	RD301 except *rad52*Δ::*hisG/rad52*Δ::*hisG*	YMO2 × YMO9
RD305	RD301 except *rad51*Δ::*hisG/rad51*Δ::*hisG*	YMO6 × YMO8
RD306	RD301 except *rad50*Δ::*hisG/rad50*Δ::*hisG*	YMO4 × YMO7
RD308	RD301 except *rad52*Δ::*hisG/rad52*Δ::*hisG rad51*Δ::*kan*MX/*rad51*Δ::*kan*MX	YMO50 × YMO51
RD309	RD301 except *rad52*Δ::*hisG/rad52*Δ::*hisG rad50*Δ::*kan*MX/*rad50*Δ::*kan*MX	YMO52 × YMO53

[a] *III*-205::*URA3* signifies that the *URA3* fragment was inserted at position 205 kb on chromosome III.
[b] *III*-314::*ADE2* signifies that the *ADE2* fragment was inserted at position 314 kb on chromosome III.
[c] *kan*MX indicates the 6His-2MYC-loxP-*kan*MX-loxP module derived from plasmid pU6H2MYC (De Antoni and Gallwitz 2000).

tion of the *URA3* marker at the *III*-205 locus in YMO1, YMO5, and YMO3 was performed as described for YKU34 (Hiraoka *et al.* 2000) and the resulting strains were designated as YMO9, YMO8, and YMO7, respectively. In the case of YMO9, pMO317, which bears a wild-type *RAD52* gene, was cotransformed with the *URA3* fragment, and *rad52* cells lacking pMO317 were selected as Lys$^-$ clones afterward. Diploid strains RD304, RD305, and RD306 are heterozygous for three markers on chromosome III, *LEU2*, *III*-205::*URA3*, and *III*-314::*ADE2*, and are homozygous for the *rad52*, *rad51*, and *rad50* mutations, respectively. *rad50*Δ *rad52*Δ or *rad51*Δ *rad52*Δ double-mutant strains were constructed as follows. *RAD50* or *RAD51* deletion fragments consisting of the 6His-2MYC-loxP-*kan*MX-loxP module flanked by 75 bp of *RAD50* or *RAD51* upstream and downstream sequences, respectively, were obtained by PCR using pU6H2MYC as a template, as described (De Antoni and Gallwitz 2000). The fragments were transformed into the *rad52* strains YMO2 and YMO9 in the presence of pMO317. Cells lacking pMO317 were selected as Lys$^-$ clones afterward. YMO2 *rad51* and *rad50* derivatives were designated as YMO50 and YMO52, and YMO9 derivatives were designated as YMO51 and YMO53, respectively. Diploid strains RD308 and RD309 are heterozygous for the three markers on chromosome III and are homozygous for the *rad51 rad52* and *rad50 rad52* double mutations, respectively. *E. coli* DH5α was used for all plasmid manipulations.

Analysis of LOH events: Analysis of LOH events was performed as described previously for strain RD301 (Hiraoka *et al.* 2000), with minor modifications. For all strains examined, freshly mated diploid cells were precultured at 30° in SC medium depleted for uracil, leucine, and adenine until midlog phase (1.0×10^6–1.0×10^7 cells/ml). Approximately 100 cells from the preculture were inoculated into a series of culture tubes with 5 ml of YPAD medium supplemented with 20 μg/ml uracil and incubated at 30° until they reached a concentration of ~5.0×10^7 cells/ml (~21 generations). After appropriate dilution and sonication, cells were spread on YPD, 5-FOA, 5-FOA leucine-depleted, and 5-FOA leucine- and adenine-depleted plates, and colonies were counted after incubation at 30° for 3–5 days. At least 16 independent experiments were performed to determine the median frequencies of LOH. For statistical evaluation of the data, we compared the hinge spread (between lower and upper hinges, that is, 25 and 75% points) and the inner fences (between ±1.5-fold points of the hinge spread from the hinges) of the determined frequencies. The inner fence is supposed to include ~98% of the population. 5-FOA-resistant (5-FOA^r) clones were classified according to their phenotypes and their chromosome III structure, as assessed by pulsed-field gel electrophoresis (PFGE), Southern hybridization, and PCR (Figure 1). The frequency of 5-FOA^r Leu$^-$ clones was determined by subtracting the median frequency of 5-FOA^r Leu$^+$ clones from that of 5-FOA^r cells. Similarly, the frequency of 5-FOA^r Leu$^+$ Ade$^-$ clones was determined by subtracting the median frequency of 5-FOA^r Leu$^+$ Ade$^+$ clones from that of 5-FOA^r Leu$^+$ cells. The validity of these methods to estimate the frequencies was confirmed pre-

viously (Hiraoka *et al.* 2000). Three patterns could be distinguished by PFGE and Southern blotting: (i) two normal-sized chromosomes III, (ii) one or more copies of an aberrant-sized chromosome III accompanied by a normal copy, and (iii) monosomy for chromosome III. Among the aberrant chromosomes, deletion of sequences between the *MAT-HMR* loci could be detected by PCR with primers encompassing these loci. Intragenic mutations were identified by sequencing the amplified *URA3* marker.

Analysis of LOH events accompanied by *ADE2* homozygosis: *ADE2* homozygosis in *rad50* cells was detected by PCR with primers specific to the *III*-314 locus that distinguish between the absence (wild-type *III*-314) and the presence (*III*-314::*ADE2*) of the *ADE2* insert. Both PCR fragments could be amplified from the original diploid (RD306) just after crossing. When PCR was performed on nonselected clones after cultivating the cells under the same conditions as for measurement of LOH, clones having only the *III*-314::*ADE2* allele (hence, probably *ADE2/ADE2*) were detected at a frequency of up to 3.2×10^{-2} in five independent experiments. The same PCR was used to analyze the structure of the *III*-314 locus in 5-FOA^r Leu$^+$ Ade$^+$ clones. The clones with only the *III*-314::*ADE2* allele (*ADE2/ADE2* or *ADE2/0*) could have undergone the *ADE2* homozygosis and the types of recombination that had caused LOH were inferred as follows. For clones with two normal-sized chromosomes, the ratio of gene conversion to allelic recombination was estimated as the ratio of the frequency of gene conversion among 5-FOA^r Leu$^+$ *ADE2/III*-314 clones (8.3×10^{-6}, Table 6) to the frequency of allelic crossing over among 5-FOA^r Leu$^+$ Ade$^-$ clones (4.5×10^{-4}, Table 4). Thus, 1.8% of the *ADE2/ADE2* clones were classified as resulting from gene conversion and the remaining majority was classified as being due to allelic crossing over. Similarly, *MAT-HMR* deletions among the clones fell into two classes based on the ratio of the frequency of intrachromosomal *MAT-HMR* deletion among 5-FOA^r Leu$^+$ *ADE2/III*-314 clones (5.6×10^{-6}, Table 6) to that of *MAT-HMR* unequal crossing over among 5-FOA^r Leu$^+$ Ade$^-$ clones (1.5×10^{-5}, Table 4). For aberrant chromosomes other than those with *MAT-HMR* deletions, all 10 clones identified among the Ade$^+$ clones (Table 6) were classified as having undergone ectopic crossing over because such aberrant chromosomes were identified only as interchromosomal events among 5-FOA^r Leu$^+$ Ade$^-$ clones (Table 4), but not as intrachromosomal events among 5-FOA^r Leu$^+$ *ADE2/III*-314 clones (Table 6). As for three monosomic 5-FOA^r Leu$^+$ Ade$^+$ clones (Table 4), the frequency of allelic crossing over among *ADE2/ADE2* clones and that of total gene conversion, accompanying *ADE2* homozygosis or not, was applied to estimate which type of allelic recombination was accompanied by the chromosome loss.

PFGE: PFGE analysis of chromosomes was performed as previously described (Hiraoka *et al.* 2000). Electrophoresis was carried out with 1% PFGE-certified agarose (Bio-Rad, Hercules, CA) in 0.5× TBE buffer at 14°, using a CHEF Mapper XA pulsed-field electrophoresis system (Bio-Rad).

Southern blotting: Transfer of chromosomal DNA fragments and detection by hybridization were performed as previously described (Hiraoka *et al.* 2000). Hybridized probes were detected with the Gene Images labeling and detection system (Amersham Pharmacia, Buckinghamshire, UK) according to the supplier's protocols. Probes were obtained by amplification of the indicated loci. Chromosome III and its derivatives were visualized with a pair of probes corresponding to two regions on the left arm of chromosome III, *III*-54 and *III*-102, as previously described (Hiraoka *et al.* 2000).

PCR procedures: PCR was performed under standard conditions with *rTaq* and *Ex Taq* DNA polymerases (Takara) as previously described (Hiraoka *et al.* 2000). *Z-Taq* DNA poly-

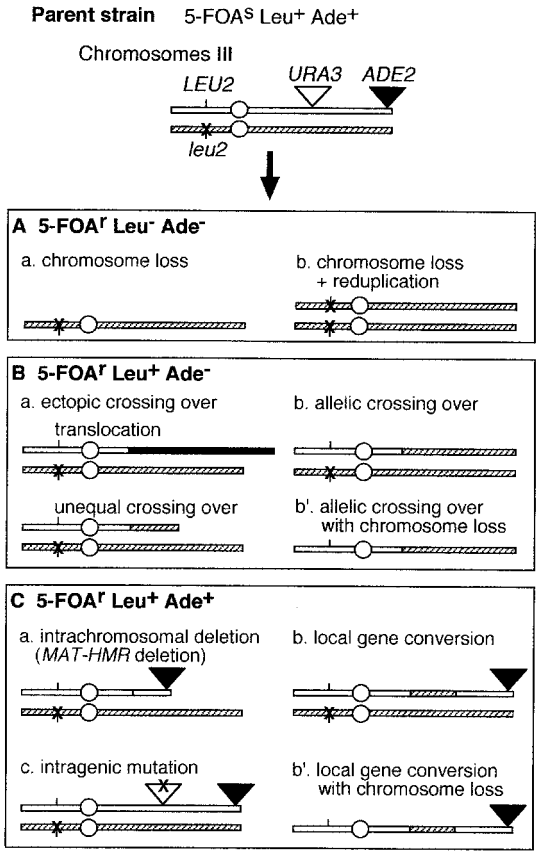

Figure 1.—Assay system to screen and classify genetic events leading to LOH. A chromosome III pair in the parent strain (above arrow) and their possible alterations in 5-FOA^r clones (below arrow) are illustrated with the relative positions of the three markers used for the analysis. The 5-FOA^r clones are classified according to their phenotypes (A–C) and their chromosome III structure (a–c), as assessed by PFGE, Southern hybridization, and PCR. (A) 5-FOA^r Leu$^-$ Ade$^-$ clones arise due to loss of the entire chromosome with the markers (a), and the remaining chromosome may undergo reduplication afterward (b). (B) 5-FOA^r Leu$^+$ Ade$^-$ clones arise from interchromosomal recombination: (a) clones with aberrant-sized chromosomes result from ectopic crossing over, either unequal crossing over or translocation; (b) clones with two normal-sized chromosomes III result from allelic crossing over. (C) 5-FOA^r Leu$^+$ Ade$^+$ clones include the following three types of events: (a) clones with aberrant-sized chromosomes arise through intrachromosomal rearrangements; clones with two normal-sized chromosomes III, as indicated by PFGE, could arise through either local gene conversion (b) or mutation of the *URA3* marker (c). The last two events can be distinguished by PCR analysis of the *URA3* insert locus. Clones monosomic for chromosome III are found among 5-FOA^r Leu$^+$ Ade$^-$ clones (B) or 5-FOA^r Leu$^+$ Ade$^+$ clones (C), where the remaining chromosome is a recombinant that arose by allelic crossing over (B-b′) or gene conversion (C-b′) between homologs. Open bars, segments of chromosome III originally harboring the markers; hatched bars, segments of the homologous chromosome III; solid bars, segments translocated from another chromosome; circles, centromeres; open triangle, the *URA3* insert at *III*-205; solid triangles, the *ADE2* insert at *III*-314; vertical lines, the positions of intrinsic *LEU2* loci; vertical lines marked with a cross, the *leu2* allele; a cross on an open triangle, an intragenic mutation inactivating the *URA3* insert.

merase (Takara) was used for breakpoint analysis of aberrant chromosomes under the conditions recommended by the supplier. Quantitative PCR analysis of *URA3*-inserted locus (*III*-205) was performed as previously described (Hiraoka *et al.* 2000). All primers used in this study were supplied by Griner Japan (Tokyo). The primers used to analyze chromosome III loci were previously described (Hiraoka *et al.* 2000) and are as follows: for the *III*-205 locus, d3W205 and d3C205; for a control locus on the left arm, d3W102 and d3C102; for the *III*-314 locus, d3W312 and d3C314; for the *MAT-HMR* deletion, d3W197 and d3C294.

Breakpoint analysis of aberrant chromosomes: For the identification of breakpoints, aberrant chromosomes were compared to those previously analyzed and their structures were examined by PCR with an appropriate primer set encompassing the putative breakpoint. For aberrant chromosomes of novel structure, the rearranged region on chromosome III was determined by a PCR-based method that determines the ploidy of multiple loci on chromosome III, as previously described (Umezu *et al.* 2002), with the following modifications: (1) genomic DNA was extracted from PFGE agarose plugs with the QIAquick gel extraction kit and the equivalent amount of DNA purified from plugs containing 1.3×10^5 cells was used as a template in 25 μl of reaction mixture, and (2) the PCR program consisted of an initial incubation at 95° for 1 min followed by 22 cycles of 92° for 1 min, 60° for 1 min, and 72° for 1 min. On the basis of the results of this analysis, the region including the breakpoint was amplified by PCR for clones 145 and 152, obtained in *rad52* mutants. The primers used were d3W168 (5′-CCACCAGTAGCATTCTTCTGTATCTG) and d3W84-2 (5′-GATAATACACCCTCCATTGATACGG). For clones 153 and 154, a translocation breakpoint was detected at ~3.5 kb distal to the *MAT***a** locus and its precise position was determined by a modified rapid amplification of cDNA 5′-end (5′-RACE) method, as follows:

1. Single-stranded DNA (ssDNA) including the breakpoint was synthesized by primer extension from the *MAT***a** locus toward the telomere. The reaction was carried out in the standard PCR mixture with the primer d3W200-a-2 (5′-GGC ATTACTCCACTTCAAGTAAGAGTTTGG). The reaction program consisted of an initial incubation at 95° for 1 min, followed by 80 cycles of 92° for 30 sec, 59° for 30 sec, and 72° for 4 min.
2. Homopolymeric dC-tails were added to the 3′ end of the newly synthesized ssDNA by terminal deoxynucleotidyl transferase (TdT; GIBCO BRL, Life Technologies, Rockville, MD). The reaction mixture (25 μl) contained 170 pg ssDNA, 0.1 M potassium cacodylate (pH 7.2), 2 mM $CoCl_2$, 200 μM dithiothreitol, 200 μM dCTP, and 10 units of TdT and was incubated for 30 min at 30°.
3. The tailed ssDNA was used as a template for the amplification of double-stranded DNA. The primers used were d3W204-2 (5′-TTATAACTGTTAACTCATCTGTTTCCTGC), which should hybridize to sequences ~200 bp upstream of the breakpoint, and the RACE adapter (5′-GGCCACGC GTCGACTAGTACGGGIIGGGIIGGGIIG).
4. The second PCR was carried out using the first PCR product as a template with the primers d3W204-2 and RACE UAP (5′-GGCCACGCGTCGACTAGTACG). The PCR product was sequenced after purification with the QIAquick PCR purification kit (QIAGEN). DNA sequencing was carried out by the dye terminator method using BigDye terminator cycle sequencing kits (PE Applied Biosystems, Foster City, CA) with a capillary sequencer (ABI PRISM310, PE Applied Biosystems). Comparison of DNA sequences was performed with GeneWorks software (version 2.5.1, Oxford Molecular Group).

RESULTS

Outline of the LOH assay: We have analyzed the spontaneous LOH events that lead to functional inactivation of the hemizygous *URA3* marker inserted at the center of the right arm of chromosome III (the *III*-205 locus) in *S. cerevisiae* diploids (Figure 1). *URA3* marker inactivation or loss can be identified by 5-FOA^r. Thus, the frequency of LOH events was determined by selecting 5-FOA^r progeny. Two additional markers on the same chromosome, the telomere-proximal *ADE2* marker on the right arm and the *LEU2* marker on the left arm, allow chromosome rearrangements associated with LOH to be monitored by examining the Ade and Leu phenotypes of 5-FOA^r clones. In addition to genetic characterization, the structure of chromosome III in LOH clones was directly analyzed by PFGE and PCR. A combination of these analyses allows a wide variety of LOH events to be identified, as diagrammed in Figure 1.

The data obtained from an analysis of a wild-type (Rad$^+$) strain by this assay provide a baseline for evaluating the effects of homologous recombination (Hiraoka *et al.* 2000). In Rad$^+$ cells, LOH events occur at a frequency of 1.2×10^{-4} and the majority of events are chromosome loss (Figure 1A-a), allelic crossing over (Figure 1B-b), and alterations in chromosome size (Figure 1, B-a and C-a). Chromosomes of aberrant size arise by interchromosomal crossing over between ectopic sequences, creating unequal crossing over and translocation events (Figure 1B-a), or by intrachromosomal rearrangement (Figure 1C-a). In Rad$^+$ cells, ectopic crossing over primarily involves recombination between Ty1 elements at various genomic locations, while intrachromosomal events exclusively involve deletion particular to chromosome III, namely a deletion between the *MAT* and *HMR* loci (Umezu *et al.* 2002). About 6% of allelic crossing-over events were accompanied by chromosome loss (Figure 1B-b′), and the two events are likely to have occurred in a concerted manner on the basis of the frequencies of each event. The frequency of local gene conversion involving the *URA3* marker (Figure 1C-b) is two orders of magnitude lower than that of allelic crossing over (Figure 1B-b), and mutation within the marker (Figure 1C-c) is rarely detected. For the recombination events detected in our assay, the mechanisms that underlie the processes could be explained by several pathways of homologous recombination, including reciprocal crossing over, BIR, and SSA (see DISCUSSION). An advantage of our assay is that the various genetic alterations detected all occurred within the same population analyzed.

The frequency of LOH is significantly increased in all of the *rad* mutants and most events lead to chromosome loss: The diploid strains for LOH analysis were constructed by mating haploid YKU23 and YKU34 derivatives that have deletions of *RAD50*, *RAD51*, or *RAD52*; both *RAD50* and *RAD52*; or both *RAD51* and *RAD52*

TABLE 2

Median frequencies of 5-FOA^r, 5-FOA^r Leu$^+$, and 5-FOA^r Leu$^+$ Ade$^+$ clones

	Median frequency (lower–upper hinges) $\times 10^5$					
Phenotype	Wild type[a]	*rad50*	*rad51*	*rad52*	*rad50 rad52*	*rad51 rad52*
5-FOA^r	12 (8.8–18.6)	362 (341–413)	245 (172–369)	332 (295–473)	559 (461–687)	474 (452–507)
5-FOA^r Leu$^+$	5.2 (2.7–8.3)	78 (75–83)	14 (9.4–16)	0.86 (0.53–2.5)	9.1 (6.2–11)	1.1 (0.76–2.0)
5-FOA^r Leu$^+$ Ade$^+$	0.35 (0.15–0.57)	4.6 (3.1–8.9)	2.9 (2.5–6.2)	0.29 (0.11–0.39)	0.31 (0.18–0.60)	0.33 (0.20–0.74)

The median frequencies of cells converted to 5-FOA^r, 5-FOA^r Leu$^+$, and 5-FOA^r Leu$^+$ Ade$^+$ were measured with 18, 20, 16, 16, and 16 independent cultures of *rad50*, *rad51*, *rad52*, *rad50 rad52*, and *rad51 rad52* mutants, respectively. Cells were inoculated at $\sim 10^2$ colony-forming units into 5 ml medium and the cultures were incubated for an average of 21 generations.

[a] Data for the strain RD301 were taken from the previous study (Hiraoka *et al.* 2000).

(Table 1). The resulting diploid strains are heterozygous for three markers on chromosome III, *LEU2*, *III*-205::*URA3*, and *III*-314::*ADE2*, and are homozygous for the *rad* mutations. The cells were incubated in rich liquid medium that allows for growth of LOH clones until they reach a certain titer, and aliquots were then spread on 5-FOA, 5-FOA leucine-depleted, and 5-FOA leucine- and adenine-depleted plates to allow for quantification of the frequency of LOH (Tables 2 and 3, Figure 2). As shown in Figure 2, these values fluctuated among experiments and we used the median rather than the arithmetical mean (Table 2) to express the frequency of LOH events because the latter is overly influenced by the jackpot effect. We evaluated LOH events on the basis of the median frequency rather than on the basis of the rate calculated from the frequency, because the growth rate of some LOH clones was more reduced than that of other clones or parental cells (Hiraoka *et al.* 2000). The frequency of 5-FOA^r Leu$^-$ clones (Figure 1A) was determined by subtracting the median frequency of 5-FOA^r Leu$^+$ clones from that of 5-FOA^r cells, and similarly, the frequency of 5-FOA^r Leu$^+$ Ade$^-$ clones (Figure 1B) was determined by subtracting the median frequency of 5-FOA^r Leu$^+$ Ade$^+$ clones from that of 5-FOA^r Leu$^+$ cells (Table 3; see materials and methods).

For all the mutant strains, total LOH frequencies (frequencies of 5-FOA^r clones) were increased significantly, 20- to 47-fold, compared to that for the isogenic wild-type strain, and the majority of LOH clones exhibited a 5-FOA^r Leu$^-$ phenotype indicative of loss of the entire chromosome (Table 3 and Figure 2). Notably, in *rad52* mutant strains with or without *rad50* or *rad51* mutations, almost all of the clones (98% or more) showed a chromosomal loss phenotype. Twenty 5-FOA^r Leu$^-$ clones from each of the single *rad* mutants were confirmed to be monosomic for chromosome III by PFGE and Southern analysis. One exceptional *rad52* clone was homozygous for normal-sized chromosome III. PCR genotyping of several loci over chromosome III showed that the two chromosomes in the clone had the same structure and that they lacked the *LEU2*, *URA3*, and *ADE2* markers, suggesting that the LOH event was due to chromosome loss followed by reduplication of the remaining chromosome (Figure 1A-b). Thus, in all of the *rad* mutants, the most prominent LOH event was chromosome loss. The frequencies of chromosome loss were statistically comparable among all the *rad* mutants, including the *rad50 rad52* and *rad51 rad52* double mutants (Table 3 and Figure 2). These results clearly indicate that homologous recombination significantly sup-

TABLE 3

Estimated frequencies of LOH classes A–C

		Estimated frequency $\times 10^5$ (class distribution, %)					
Class[a]	Phenotype	Wild type[b]	*rad50*	*rad51*	*rad52*	*rad50 rad52*	*rad51 rad52*
A	5-FOA^r Leu$^-$	6.8 (57)	284 (78)	231 (94)	331 (99.7)	550 (98.3)	472 (99.5)
B	5-FOA^r Leu$^+$ Ade$^-$	4.9 (41)	73 (20)	11 (4.5)	0.56 (0.17)	8.8 (1.6)	0.81 (0.17)
C	5-FOA^r Leu$^+$ Ade$^+$	0.35 (2.9)	4.6 (1.3)	2.9 (1.2)	0.29 (0.087)	0.31 (0.056)	0.33 (0.069)
Total	5-FOA^r	12 (100)	362 (100)	245 (100)	332 (100)	559 (100)	474 (100)

The frequency of 5-FOA^r Leu$^-$ clones was calculated by subtracting the frequency of 5-FOA^r Leu$^+$ clones from that of 5-FOA^r cells. Similarly, the frequency of 5-FOA^r Leu$^+$ Ade$^-$ clones was calculated by subtracting the frequency of 5-FOA^r Leu$^+$ Ade$^+$ clones from that of 5-FOA^r Leu$^+$ cells. Numbers in parentheses represent the proportion of individual classes to total 5-FOA^r events in the strain.

[a] Classification of 5-FOA^r clones together with their phenotypes is as shown in Figure 1.

[b] Data for the strain RD301 were taken from the previous study (Hiraoka *et al.* 2000).

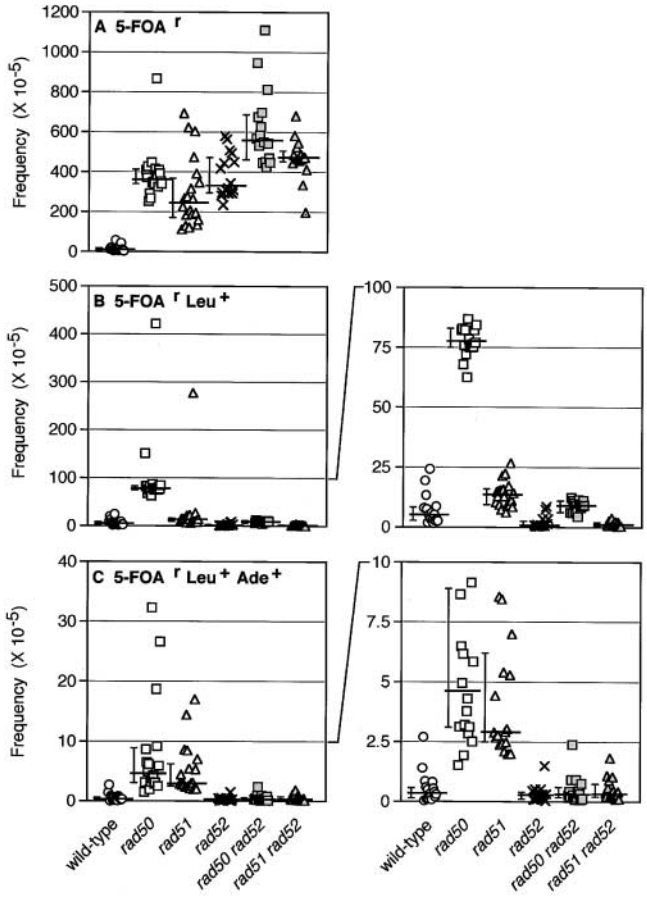

FIGURE 2.—Scatter plot of the frequencies of 5-FOA^r, 5-FOA^r Leu$^+$, and 5-FOA^r Leu$^+$ Ade$^+$ clones derived from *rad* mutants. Symbols represent the frequencies of 5-FOA^r (A), 5-FOA^r Leu$^+$(B), and 5-FOA^r Leu$^+$ Ade$^+$ (C) clones measured within individual cultures of the indicated strains. (B and C) The indicated portion of the scatter gram is enlarged on the right. Culture numbers for each strain are shown in Table 2. Median frequencies are shown with solid bars. Hinge spreads are indicated with vertical lines segmented with bars indicating the lower and upper hinges (25 and 75% points, respectively). Data of the wild-type strain, RD301, are taken from a previous study (HIRAOKA *et al.* 2000).

presses LOH in Rad$^+$ cells and that in its absence chromosomes are destabilized and lost from the cells. The major pathway contributing to chromosome maintenance appears to require all the *RAD50*, *RAD51*, and *RAD52* functions.

On the other hand, each mutant differentially affected the frequency of 5-FOA^r Leu$^+$ clones that include various types of LOH events other than chromosome loss (Table 2 and Figure 2): the frequency was enhanced significantly in *rad50* mutants and to lesser extent in *rad51* mutants, while it was decreased in *rad52* mutants. LOH events other than chromosome loss were identified by the strategy shown in Figure 1 for *rad50*, *rad51*, and *rad52* single-mutant strains: 5-FOA^r Leu$^+$ clones were classified according to phenotype (Table 3) and their alterations in chromosome III structure, as assessed by PFGE, Southern hybridization, and PCR with ≥80 clones randomly selected from multiple experiments in each strain (Tables 4, 6, and 7). On the basis of these results, the proportion of individual events in each class was determined, and this value was used to calculate the frequency of each event, as shown in Tables 4, 6, and 7. The frequencies of LOH events in the *rad* mutants are summarized in Table 8, and Figure 3 indicates the fold decrease or increase in the frequency of each event relative to that in Rad$^+$ cells. The distribution of LOH events was quite different among the three *rad* strains, as described below.

Disruption of the *RAD52* gene reduces the frequencies of all types of recombination: The frequencies of all forms of recombination were decreased to a variety of extents in *rad52* mutants compared with Rad$^+$ cells (Figure 3). For allelic recombination, the frequency of crossing over was decreased 10-fold whereas the frequency of gene conversion was decreased slightly, if at all. For intrachromosomal recombination, all 13 isolates exhibited, as in Rad$^+$ cells, a deletion of sequences between the *MAT* and *HMR* loci (Table 4), with an overall decrease in frequency of ~3-fold. The frequency of aberrant chromosomes resulting from ectopic crossing over was decreased ~6-fold. These *RAD52*-independent interchromosomal rearrangements could be due to other mechanisms, such as NHEJ, that may substitute for homologous recombination. To examine this possibility, we determined the site of the breakpoints of all aberrant chromosomes identified in *rad52* mutants (Table 5). This analysis indicated that all of them arose through unequal crossing over or translocation and that the sequences utilized for rearrangement were repetitive sequences of sufficient length for homologous recombination, except for one case. In three clones (151, 328, and 146) the breakpoints were in the same 5.6-kb Ty1 elements as aberrant chromosomes observed in Rad$^+$ cells (UMEZU *et al.* 2002). The *MAT-HMR* repeat sequences were involved in recombination between the homologs in one case (clone 342), whereas an aberrant chromosome in two clones (145 and 152, which were isolated from the same culture and hence probably siblings) consisted of a fusion between a Ty1 element in the *CEN3-URA3* interval and the Ty2 element on the left arm of chromosome III, sharing ~3 kb of homology in the inverted orientation. In contrast to these breakpoints found in repetitive sequences, an aberrant chromosome in the remaining two clones (153 and 154, which were also probably siblings) had breakpoints in 4-bp sites of microhomology at the *III*-204 locus of chromosome III and the *XII*-368 locus of chromosome XII. Accordingly, we conclude that the majority of chromosome rearrangements found in *rad52* mutants were caused by mechanisms involving homologous recombination, both allelic and ectopic, and that all types of homologous recombination were decreased by this mutation, consistent with known roles for Rad52. Nonethe-

TABLE 4

Classification of 5-FOA^r Leu$^+$ Ade$^-$ clones and 5-FOA^r Leu$^+$ Ade$^+$ clones based on the copy number and the size abnormality of chromosome III

Strain	Phenotypes	Frequency $\times 10^5$	Estimated frequency $\times 10^5$ (no. of clones identified/no. of clones analyzed): authentic chromosome III:aberrant chromosome III[b]			
			2:0	1:1 (*MAT-HMR*Δ)[c]	1:≥1 (non-*MAT-HMR*Δ)[d]	1:0
Wild type[a]	5-FOA^r Leu$^+$ Ade$^-$	4.9	4.0 (115/140 = 0.82)	<0.035 (0/140 < 0.0071)	0.63 (18/140 = 0.13)	0.25 (7/140 = 0.05)
	5-FOA^r Leu$^+$ Ade$^+$	0.35	0.039 (11/98 = 0.11)	0.31 (87/98 = 0.89)	<0.0036 (0/98 < 0.010)	<0.0036 (0/98 < 0.010)
rad52	5-FOA^r Leu$^+$ Ade$^-$	0.56	0.38 (27/40 = 0.68)	0.014 (1/40 = 0.025)	0.11 (8[e]/40 = 0.20)	0.056 (4/40 = 0.10)
	5-FOA^r Leu$^+$ Ade$^+$	0.29	0.19 (26/40 = 0.65)	0.095 (13/40 = 0.33)	<0.0073 (0/40 < 0.025)	0.0073 (1[f]/40 = 0.025)
rad51	5-FOA^r Leu$^+$ Ade$^-$	11	1.6 (8/55 = 0.15)	<0.19 (0/55 < 0.018)	8.8 (45/55 = 0.82)	0.39 (2/55 = 0.036)
	5-FOA^r Leu$^+$ Ade$^+$	2.9	0.18 (3/50 = 0.060)	2.7 (46/50 = 0.92)	0.058 (1/50 = 0.020)	<0.058 (0/50 < 0.020)
rad50	5-FOA^r Leu$^+$ Ade$^-$	73	45 (31/50 = 0.62)	1.5 (1/50 = 0.02)	18 (12/50 = 0.24)	8.8 (6[g]/50 = 0.12)
	5-FOA^r Leu$^+$ Ade$^+$	4.6	2.8 (30/50 = 0.60)	0.65 (7/50 = 0.14)	0.93 (10/50 = 0.20)	0.28 (3/50 = 0.060)

The frequency of each class was obtained by multiplying the frequency of 5-FOA^r Leu$^+$ Ade$^-$ cells or of 5-FOA^r Leu$^+$ Ade$^+$ cells by the corresponding ratio of the clones with the indicated chromosome pattern shown in parentheses. For the analysis of chromosome pattern, the indicated number of the clones was randomly chosen from four to five independent cultures of each *rad* mutant strain. 5-FOA^r Leu$^+$ Ade$^+$ clones carrying two authentic chromosomes III were further classified on the basis of whether or not the clones had the *URA3* marker sequence, which provides a way to distinguish intragenic mutations from allelic recombination (see text for details). The number of clones having the *URA3* marker sequences is as follows: in wild type, 2 out of 98; in *rad52*, 22 out of 26; in *rad51*, all 3; and in *rad50*, none. The remaining clones without the *URA3* marker were classified as allelic recombination. The frequencies of these events are indicated in Tables 7 and 8.

[a] Data for the strain RD301 were taken from the previous study (Hiraoka *et al.* 2000).

[b] Chromosome pattern in the clones was analyzed by PFGE and Southern blotting. Copy numbers of the normal-sized chromosome III and that of the aberrant-sized one are indicated.

[c] Aberrant chromosomes with deletions between *MAT* and *HMR* loci that were detected by PCR as described in materials and methods.

[d] Aberrant chromosomes other than those with *MAT-HMR* deletions.

[e] A clone that had an aberrant chromosome carrying only the telomeric half of the left arm of chromosome III, which could not be defined as ectopic recombination in Tables 5 and 8 because it did not obey our definition for aberrant chromosomes III. A similar type of aberrant chromosome was also found in the analysis of wild-type cells (Umezu *et al.* 2002).

[f] This monosomic clone had a mutation in the *URA3* marker on chromosome III, 260 (AT → CG; Table 7), and hence the LOH event in the clone was classified as an intragenic mutation.

[g] A clone that had both *LEU2* and *leu2* alleles, which made the determination of a LOH event in the clone ambiguous. Hence, the clone was not included in the results shown in Table 8.

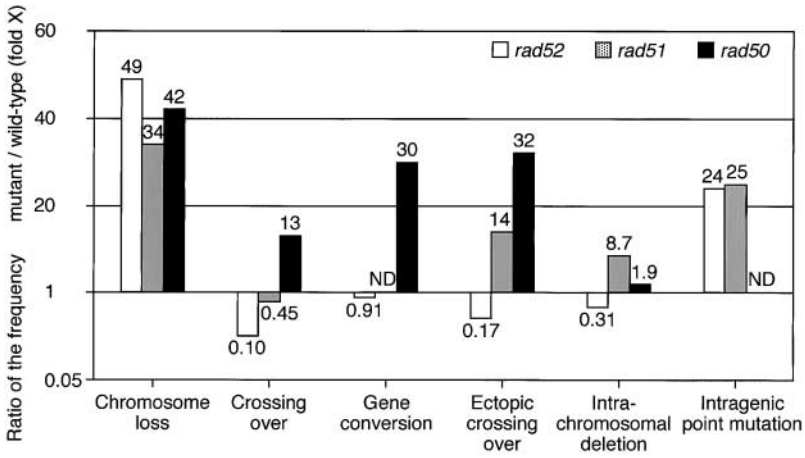

FIGURE 3.—Fold increase and decrease of the frequency of LOH events in the *rad* mutants relative to that in Rad$^+$ cells. The bar graphs represent the ratios of the frequency of individual events in the *rad* mutants relative to that of wild-type cells. Values of the ratios are shown on the top of each bar.

less, *rad52* deficiency was insignificant for some LOH events in this analysis.

Clones monosomic for chromosome III were identified among both 5-FOA^r Leu$^+$ Ade$^-$ clones and 5-FOA^r Leu$^+$ Ade$^+$ clones from *rad52* mutants (Table 4), which can be distinguished from 5-FOA^r Leu$^-$ monosomic clones (Figure 1). Because the frequency of chromosome loss itself is significant in *rad52* mutants, it is difficult to tell whether chromosome loss occurred in concert with allelic recombination, as we concluded for Rad$^+$ cells (HIRAOKA *et al.* 2000). This caveat is applicable for similar clones derived from *rad51* or *rad50* mutants as well.

The frequency of aberrant chromosomes is increased in *rad51* mutants: Disruption of the *RAD51* gene resulted in a distribution of recombination events different from that in *rad52* mutants and Rad$^+$ cells (Figure 3 and Table 8). In *rad51* mutants, the frequency of allelic crossing over was decreased only ~2-fold relative to Rad$^+$ cells. Gene conversion was not observed among 50 5-FOA^r Leu$^+$ Ade$^+$ clones (Table 4). On the other hand, the frequency of ectopic recombination was clearly increased: 14-fold for ectopic crossing over and 8.7-fold for intrachromosomal deletion, as compared to Rad$^+$ cells. All but one of 47 isolates with intrachromosomal deletions had lost sequences between the *MAT-HMR* loci (Table 4). The remaining clone exhibited a ploidy pattern indicative of an intrachromosomal deletion between the Ty insertion hotspots on chromosome III (UMEZU *et al.* 2002). Nine of 45 isolates that had undergone ectopic crossing over were analyzed, and all of them were shown to have breakpoints in the same Ty1 elements or at least to display the same patterns of ectopic crossing over as seen in Rad$^+$ cells, with respect to ploidy. Thus, both intra- and interchromosomal ectopic recombination likely occurred between homologous sequences in *rad51* mutants. These results indicate that the *rad51* mutation increases homologous recombination involving ectopic but not allelic sites.

The frequencies of all types of recombination are increased in *rad50* mutants: During the analysis of 5-FOA^r Leu$^+$ Ade$^+$ clones in *rad50* mutants, we noted that 10 of 50 clones (20%) had size aberration of chromosome III not attributable to the *MAT-HMR* deletion (Table 4) and that some aberrant chromosomes were longer than normal chromosome III, indicating that they did not result from intrachromosomal LOH events. Breakpoint analysis of these 10 aberrant chromosomes revealed that 7 arose through either unequal crossing over or translocation, which had been assumed to give rise only to 5-FOA^r Leu$^+$ Ade$^-$ clones (Figure 1B-a). The remaining three exhibited a more complex structure with accompanying amplification, similar to interchromosomal rearrangements observed in some Rad$^+$ cells (UMEZU *et al.* 2002). One plausible explanation for these findings is that the hemizygous *ADE2* marker had become homozygous prior to a LOH event at a relatively high frequency (*ADE2*-homozygosis, Figure 4), and subsequent interchromosomal events led to the 5-FOA^r Leu$^+$ Ade$^+$ LOH phenotype. In fact, cells homozygous for the *ADE2* insert accumulated in the *rad50* population at a frequency of up to 3.2×10^{-2}, as measured in five independent experiments for cells cultivated under the same conditions used to monitor LOH (MATERIALS AND METHODS). This frequency is high enough to bias the analysis of 5-FOA^r Leu$^+$ Ade$^+$ clones. We also found a high incidence of *ADE2* homozygosis in our previous analysis of the *sgs1* mutant, which exhibits a hyperrecombination phenotype, whereas in Rad$^+$ cells, the rarity of the event did not affect the LOH analysis (AJIMA *et al.* 2002).

To determine the nature of LOH events within 5-FOA^r Leu$^+$ Ade$^+$ clones, the genotype of the locus at which *ADE2* was inserted (*III*-314) was analyzed by PCR using primers that distinguish the presence (*III*-314::*ADE2*) from the absence (wild-type *III*-314) of the marker. As shown in Table 6, the clones could be classified into two types: those with only the *III*-314::*ADE2* allele (*ADE2/ADE2* or *ADE2/0*) and those with both alleles (*ADE2/III*-314). The *ADE2/III*-314 clones likely arose from the original strain, which was hemizygous for the *ADE2* marker (Figure 1C), whereas the clones with only the *III*-314::*ADE2* allele could have undergone *ADE2* homozygosis and we could not identify which recombination

TABLE 5

Interchromosomal aberrant chromosomes identified in *rad52* mutants

Clone name	Size difference (kb) PFGE/map[a]	Type of recombination	Clones identified (cultures)[b]	Elements or sequences at the breakpoints[c]
151, 328	−60/−72	Translocation	2 (2)	Ty1-4, Ty1-1
146	+370/+380	Translocation	1 (1)	Ty1-2, (VII) Ty1-1
342	−80/−94	Unequal crossing over	1 (1)	*MAT*, *HMR*
145, 152	−50/−64	Translocation	2 (1)	Ty1-4, Ty2
153, 154	+1200 − +2200/∼+2000	Translocation	2 (1)	*III*-204 ATGAATTAAA**GGCG**CCTATAGCCC Joint ATGAATTAAA**GGCG**TCCCCCTGTGG *XII*-368 CTAAATCATC**GGCG**TCCCCCTGTGG

[a] The difference in size between the aberrant chromosome and the 330-kb wild-type chromosome III is indicated. The size of the aberrant chromosome, indicated before the slash, was determined by PFGE of the clone. The expected size of the aberrant chromosome, indicated after the slash, was calculated on the basis of the physical map derived from the SGD.

[b] The number of clones is shown together with the number of independent cultures from which the clones were isolated (indicated in parentheses). In total, 40 5-FOA^r Leu$^+$ Ade$^-$ clones from four independent cultures were analyzed.

[c] DNA elements or sequences detected at the junctions on the parental chromosomes are indicated. Ty elements are designated with the number that denotes their relative position on the chromosome (Umezu *et al.* 2002). For the Ty elements on chromosomes other than chromosome III, the number of the chromosome is indicated before the description of the element in parentheses. For clones 153 and 154, nucleotide sequences at the breakpoints are indicated; top and bottom rows indicate the sequences around the junctions on parental chromosomes, corresponding to the *III*-204 locus of chromosome III and the *XII*-368 locus of chromosome XII, respectively. The sequence in between corresponds to that of the breakpoint on the aberrant chromosome. The 4-bp homology between the breakpoints is shown in boldface type.

mechanism was responsible for LOH (Figure 4). Hence, we estimated the proportion of individual events within the clones on the basis of the defined frequency of the corresponding event in the parent strain (materials and methods), a method similar to that used in the analysis of LOH in *sgs1* mutants (Ajima *et al.* 2002). For example, the ratio of gene conversion to allelic recombination among *ADE2/ADE2* clones was estimated as the ratio of the frequency of gene conversion among 5-FOA^r Leu$^+$ *ADE2/III*-314 clones to the frequency of allelic crossing over among 5-FOA^r Leu$^+$ Ade$^-$ clones, and so on. As a result, the frequency of interchromosomal events among 5-FOA^r Leu$^+$ Ade$^+$ clones accounts for 4–5% of the corresponding events among 5-FOA^r Leu$^+$ Ade$^-$ clones, similar to the frequency of *ADE2* homozygosis directly measured in the *rad50* population. The 5-FOA^r Leu$^+$ Ade$^+$ clones obtained in *rad52* or *rad51* mutant strains were also analyzed for the status of the *III*-314 locus using the same PCR conditions, confirming that, in these mutants, all such clones were hemizygous for the *ADE2* marker.

The total frequencies of individual events in *rad50* mutants are summarized in Table 8 and Figure 3. *rad50* mutants exhibited an increase in the frequencies of all types of recombination in the LOH assay. The frequencies of allelic recombination were increased 13-fold and 30-fold for crossing over and gene conversion, respectively, compared to those in Rad$^+$ cells. The frequency of ectopic crossing over was also increased 32-fold. The frequency of intrachromosomal deletion between *MAT-HMR* was ∼2-fold higher, much lower than that for other types of recombination. Thus, the *rad50* mutation increased LOH promoted by all types of allelic and ectopic recombination involving homologous sequences. Most events were *RAD52* dependent, as seen by the large decrease in their frequency in *rad50 rad52* double mutants (Table 3 and Figure 2). The *rad50* mutation increased the *RAD52*-independent recombination as well, as shown by its higher frequency in *rad50 rad52* mutants compared to that in *rad52* mutants. In addition, *ADE2* homozygosis arising through allelic recombination was also induced in *rad50* but not in *rad51* and *rad52* mutants.

The *rad52* and *rad51* mutations increase the frequency of intragenic point mutations: In both *rad52* and *rad51* mutants, the frequency of mutations within the *URA3* insert was increased ∼25-fold compared to Rad$^+$ cells (Table 8 and Figure 3). In *rad52* mutants, LOH clones carrying the mutation were readily detected (23 of 40 5-FOA^r Leu$^+$ Ade$^+$ clones; Tables 4 and 7). While only 3 such clones were isolated out of 50 in *rad51* mutants, the frequency of 5-FOA^r Leu$^+$ Ade$^+$ clearly increased compared to wild type (Table 3 and Figure 2), allowing us to conclude that point mutation increased in *rad51* mutants. On the other hand, these were rarely found in our previous analysis of Rad$^+$ cells (2 of 98 5-FOA^r Leu$^+$ Ade$^+$ clones), where the two Rad$^+$ clones were

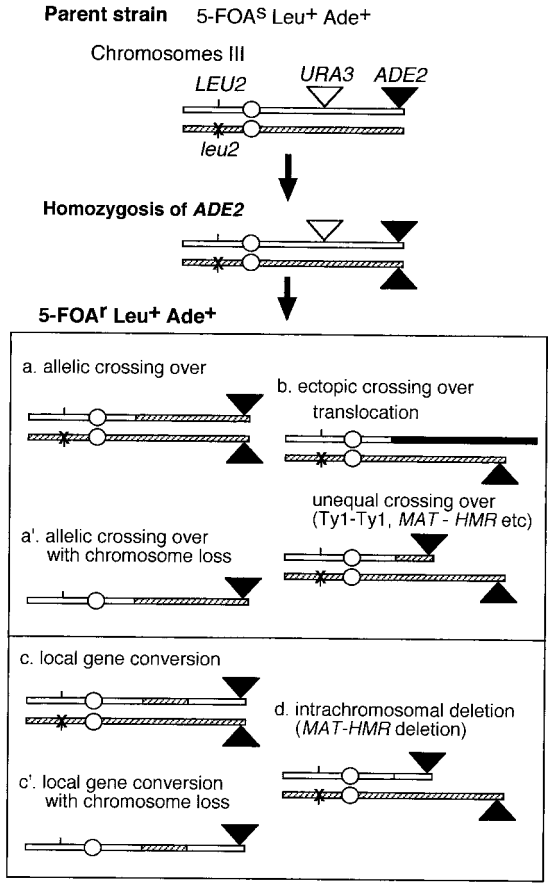

FIGURE 4.—LOH events accompanied by *ADE2* homozygosis in *rad50* mutants. The diagram shows the process of homozygosis of the *ADE2* marker in the parent strain and recombinational LOH events that may have occurred in the 5-FOA^r Leu$^+$ Ade$^+$ clones. If the events occurred in cells that had already been converted to *ADE2/ADE2*, the clones with two normal-sized chromosomes III could arise through either allelic crossing over (a) or gene conversion (c). Similarly, aberrant chromosomes in such clones could arise due to either interchromosomal or intrachromosomal recombination (b and d). Symbols are as in Figure 1.

most likely siblings and hence the contribution of point mutations in Rad$^+$ cells was probably overestimated (HIRAOKA *et al.* 2000). Accordingly, the enhancement of the intragenic mutation frequency by the *rad52* or *rad51* mutation would be >25-fold. The spectrum of mutations in the 23 isolates from *rad52* mutants is shown in Table 7. Mutations consisted of base substitutions or −1 frameshifts. It is noteworthy that three clones carried two closely spaced base substitutions; in one clone, the two mutations were separated by 1 bp, and in the other two clones, isolated from the same culture and probably siblings, the two mutations were 15 bp apart. In *rad51* mutants, 3 of 50 5-FOA^r Leu$^+$ Ade$^+$ clones had an intragenic mutation, all of which were transversion-type base substitutions (Table 7). This population is too small for a meaningful comparison with the spectrum of *rad52* point mutations. In *rad50* mutants, we identified no intragenic point mutation within LOH clones (Tables 4 and 7).

DISCUSSION

We analyzed LOH events in *rad50*Δ, *rad51*Δ, *rad52*Δ, *rad50*Δ *rad52*Δ, and *rad51*Δ *rad52*Δ homozygous diploids. The LOH assay in this study could detect a wide variety of genetic alterations, including different types of recombination as well as chromosome loss and point mutation, and hence allows for an overall view of genetic instability in the mutant strains. Most importantly, the various alterations detected occurred within the same population subjected to the analysis and we can therefore directly compare the effects of these mutations on different types of events. Generally, whereas a decrease in the frequency of a given event caused by a mutation may reflect the inactivation of pathways requiring the cognate gene function, a concomitant increase in the frequency of other events could be regarded as due to the channeling of substrates to alternative pathways.

TABLE 6

Classification of 5-FOA^r Leu$^+$ Ade$^+$ clones in *rad50* mutants based on the genotype of the *III*-314 locus

	Estimated frequency × $10^{5[b]}$ (no. of clones identified): authentic chromosome III:aberrant chromosome III[c]		
ADE2 insert[a] (genotype)	2:0	1:1 (*MAT-HMR*Δ)	1:≥1 (non-*MAT-HMR*Δ)
+ (*ADE2/ADE2* or *ADE2*/0)	1.9 (21)	0.093 (1)	0.93 (10)
± (*ADE2/III*-314)	0.83 (9)	0.56 (6)	<0.093 (ND)
Total	2.8 (30)	0.65 (7)	0.93 (10)

ND, not detected.

[a] The genotype of the *III*-314 locus, at which *ADE2* was inserted, in 5-FOA^r Leu$^+$ Ade$^+$ clones was analyzed by PCR of the region encompassing the locus. The clones were classified into two types depending on whether or not they harbored a wild-type *III*-314 allele, in addition to an *ADE2*-inserted allele (*III*-314::*ADE2*). The former is indicated as ± and the latter is indicated as +.

[b] The frequency of each class was obtained by multiplying the frequency of the clones with the indicated chromosome pattern by the ratio of the clones with the indicated genotype.

[c] Chromosome pattern in the clones is described in Table 4.

TABLE 7

Mutations identified within the *URA3* marker of LOH clones

Strain	Frequency × 10^5 (-fold)	Mutations identified (clones identified)	Base substitution					−1 frameshift
			GC → AT	AT → TA	AT → CG	GC → TA	GC → CG	
Wild type[a]	0.0071 (1)	2 (2)	0	0	0	2	0	0
rad52	0.17 (24)	26 (23)	9	4	3	5	1	4
rad51	0.18 (25)	3 (3)	0	1	0	1	1	0
rad50	<0.093 (<13)	ND	—	—	—	—	—	—

Mutations involve the following nucleotides, which are numbered relative to the start codon of the *URA3* gene. Changes are indicated in parentheses together with comments when more than one clone in the same culture or double mutations in the same clone were identified: for wild type, 332 (GC → TA) in two clones of the same culture; for *rad52*, 21 (−G), 28 (GC → CG), 89 (GC → AT), 104 (GC → TA) in two clones of the same culture, 181 (GC → AT) in five clones from two cultures, 251 (−A) in two clones of the same culture, 260 (AT → CG), 271 (GC → AT), both 297 (AT → TA) and 313 (AT → CG) in two clones of the same culture, 427 (GC → TA), 536 (AT → TA), 543 (−C), both 559 (GC → AT) and 561 (GC → AT) in the same clone, 602 (GC → TA), 624 (GC → TA), and 652 (AT → TA); for *rad51*, 286 (GC → CG), 449 (AT → TA), and 701 (GC → TA). ND, not detected.

[a] Data for the strain RD301 were taken from the previous study (Hiraoka *et al.* 2000).

The *RAD52*, *RAD51*, and *RAD50* genes are all required for chromosome maintenance: In all the mutant strains, the frequency of LOH was significantly increased and the majority of the events were chromosome loss (Table 3), indicating that homologous recombination plays a significant role in chromosome maintenance. In other words, in Rad^+ cells, the occurrence of LOH is strongly inhibited in a homologous recombination-dependent manner that likely involves recombination between sister chromatids. On the basis of this notion, the frequency of spontaneous sister chromatid recombination per unit length can be estimated as at least 25-fold higher than that of allelic recombination in wild-type cells from our analysis (Table 8). For the recombinational repair of UV- or X-ray-induced DNA damage, sister chromatids are preferred over homologous chromosomes as substrates (Kadyk and Hartwell 1992, 1993). The observation that the frequencies of chromosome loss were comparable among the *rad* mutants, including the double mutants, implies that recombination between sister chromatids requires the *RAD50*, *RAD51*, and *RAD52* functions. The critical requirement for these genes in chromosome maintenance is in clear contrast to their roles in other types of homologous recombination. This notion implies that recombinational functions must be controlled to mediate efficient and precise recombination between sister chromatids and thereby to ensure chromosome stability.

Because we measured LOH events occurring in exponentially growing cells in the absence of exogenous DNA damage, our results also suggest that recombinogenic DNA lesions arise spontaneously under normal growth conditions and that, in the absence of homologous recombination, some of them are improperly processed with eventual chromosome destruction, as has been proposed to explain the elevated level of chromosome instability in *rad52* mutants (Mortimer *et al.* 1981; Paques and Haber 1999). It is also possible that some DNA lesions are produced because of the *rad* mutations. For example, it is known that *rad50* mutants have short telomeres (Kironmai and Muniyappa 1997; Boulton and Jackson 1998; Nugent *et al.* 1998), which might be related to our observation that the *rad50* mutation caused an increase in *ADE2* homozygosis at the locus juxtaposed to a subtelomeric region. Recently, it has been recognized that specific events occurring during cell growth can trigger homologous recombination, such as the stalling or collapse of replication forks in S phase (Haber 1999; Kuzminov 1999; Cox *et al.* 2000), although the precise nature of such events remains unknown. Consistent with this, our preliminary comparison of LOH frequencies between logarithmic- and post-logarithmic-phase populations suggests that LOH events are correlated with cell growth (data not shown). Unresolved defects in the progression of replication may prevent chromosome duplication with eventual chromosome loss, in agreement with our result that defects in

TABLE 8

LOH events in *rad52*, *rad51*, and *rad50* mutants

Classes	Frequency × 10^5 (-fold)[a] [%][b]											
	Wild type[c]			*rad52*			*rad51*			*rad50*		
Loss of chromosome III	6.8	(1)	[56]	331	(49)	[99.7]	231	(34)	[94]	284	(42)	[79]
Interchromosomal recombination[d]												
Allelic crossing over	4.3	(1)	[34]	0.44	(0.10)	[0.13]	1.94	(0.45)	[0.79]	55	(13)	[15]
(with loss of chromosome III)	0.25	(1)	[2.1]	0.056	(0.22)	[0.017]	0.39	(1.6)	[0.16]	7.5	(30)	[2.1]
Ectopic crossing over	0.63	(1)	[5.5]	0.11	(0.17)	[0.034]	8.8	(14)	[3.6]	20	(32)	[5.5]
Gene conversion	0.032	(1)	[0.27]	0.029	(0.91)	[0.0088]	<0.058	(<1.8)	—	0.95	(30)	[0.26]
(with loss of chromosome III)	<0.0036	(1)	—	<0.0073	—	—	<0.058	—	—	0.084	(>23)	[0.023]
Intrachromosomal deletion[d]												
MAT-HMR deletion	0.31	(1)	[2.6]	0.095	(0.31)	[0.029]	2.7	(8.7)	[1.1]	0.58	(1.9)	[0.16]
Other deletion	<0.0036	(1)	—	<0.073	—	—	0.058	(>16)	[0.024]	<0.093	—	—
Intragenic point mutation	0.0071	(1)	[0.06]	0.17	(24)	[0.051]	0.18	(25)	[0.071]	<0.093	(<13)	—
Total	12	(1)	[100]	332	(28)	[100]	245	(20)	[100]	362	(30)	[100]

[a] Numbers in parentheses represent the ratio of the frequency of the individual events in the *rad* mutant strain relative to that of the wild type.

[b] Numbers in brackets represent the proportion of individual events to total LOH events in the strain.

[c] Data for the strain RD301 were taken from the previous study (Hiraoka *et al.* 2000).

[d] The frequencies in *rad50* mutants were adjusted on the basis of the analysis of *ADE2* homozygosis shown in Table 6 (see details in text).

homologous recombination cause a high incidence of chromosome loss. While the primary events that lead to homologous recombination can vary widely, the DNA structures that initiate recombination can be so-called two-strand lesions, such as a double-stranded end or a daughter strand gap across from a noncoding lesion (Kuzminov 1999). The frequency of chromosome loss in *rad52* mutants, that is, in the absence of the major recombination pathways, was 3.3×10^{-3} only for the 330-kb chromosome III, 1 among 32 chromosomes in yeast diploid cells with 24 Mb genomic DNA. This value is likely to reflect the minimum number of lesions on this chromosome that absolutely require homologous recombination for repair. It is noteworthy that this is a level in the presence of checkpoint responses that allows various repair processes to take place in an organized manner. Indeed, we have observed a G_2-M delay in the *rad* mutants under the conditions used to measure LOH, characterized by the accumulation of large-bud cells and a prolonged doubling time (data not shown). In *orc1-4* mutants, LOH events in this assay are significantly enhanced and augmented synergistically by the defect in the *RAD9*-dependent damage checkpoint (Watanabe *et al.* 2002). Previous studies also showed that *CDC5*-dependent checkpoint adaptation is a prerequisite for spontaneous and X-ray-induced chromosome loss in the *rad52* or *rad51* background (Galgoczy and Toczyski 2001) and that inactivation of the DNA damage checkpoint in *rad51* mutants elevates the rate of spontaneous chromosome loss (Klein 2001). For *rad50 rad52* double mutants, an additional small effect of the *rad50* mutation (Table 3 and Figure 2) might be explained by the role of the MRX complex in the DNA damage checkpoint (Grenon *et al.* 2001; Usui *et al.* 2001). Taken together, these results imply that spontaneous DNA lesions capable of triggering homologous recombination occur at a notably high frequency throughout the genome during normal cell growth.

Multiple recombination pathways and their roles in spontaneous LOH events: *rad52*, *rad51*, and *rad50* mutants each exhibited a distinct pattern of LOH although chromosome loss was the most prominent event for all three strains (Figure 3 and Table 8). These results are consistent with the notion that in mitotic cells, homologous recombination employs distinct pathways involving different subsets of genes. Accordingly, when some pathways are blocked owing to mutation, the LOH events in these cells vary depending on which alternative pathways are utilized.

RAD52-dependent and -independent recombination pathways: The decrease of all types of recombination in *rad52* mutants indicates that *RAD52*-dependent homologous recombination has a central role in generating chromosome rearrangements that lead to LOH. However, compared to the drastic reduction in heteroallelic recombination or DSB repair conferred by *rad52* mutations, as shown in previous studies (reviewed in Paques and

Haber 1999), this effect was insignificant for some types of recombination events, as found in this study. In addition, all aberrant chromosomes identified in the mutants had breakpoints within long repeats such as the *MAT* and *HMR* loci and Ty elements, apart from one case mediated by a 4-bp sequence. These results imply that, in certain situations that lead to LOH, some types of homologous recombination can take place in a *RAD52*-independent manner. Identification of the mechanism responsible for these LOH events in *rad52* mutants requires a determination of the genetic requirements for the events. These events are *RAD51* independent, as shown by their similar frequency in *rad52* and *rad51 rad52* double mutants (Table 2 and Figure 2). It has been shown that both spontaneous and DSB-induced deletions between direct repeats can occur in a *RAD52*-independent way (Klein 1995; Paques and Haber 1999). Direct repeat deletions, especially induced by DSBs, have been assumed to arise through a SSA mechanism. The 1.6-kb *MAT-HMR* and 6-kb Ty1 elements for which we detected *RAD52*-independent rearrangements should be long enough to allow for SSA-mediated deletion (Klein 1995), and hence such rearrangements might have occurred through a similar SSA mechanism.

Suppression of ectopic recombination by RAD51: In *rad51* mutants, the frequency of ectopic but not allelic recombination was increased, whereas the *rad52* mutation decreased the frequencies of all forms of recombination. All of the aberrant chromosomes analyzed in *rad51* mutants appear to have breakpoints within repetitive sequences long enough to allow homologous recombination. Thus, the *RAD51* gene appears to ensure that homologous recombination takes place between specific substrates, that is, between sister chromatids or allelic loci rather than ectopic loci. Because both BIR and SSA can occur in a *RAD51*-independent and *RAD52*-dependent way (Paques and Haber 1999), these mechanisms could be responsible for the aberrant chromosomes obtained in *rad51* mutants. In this respect, it is intriguing that human Rad52p can mediate homologous pairing *in vitro* (Kagawa *et al.* 2001). Shibata *et al.* (2001) proposed that unlike this Rad52-mediated reaction, pairing mediated by RecA-type proteins, including Rad51p, can discriminate against misaligned DNA molecules and hence can dissociate heteroduplexes formed between homologous sequences of limited length. In the absence of Rad51p, Rad52-mediated homologous pairing may occur efficiently between relatively short homologous sequences at ectopic sites, leading to an increase in chromosomal aberrations, which could account for our observations in *rad51* mutants.

The Rad51p strand exchange activity plays a key role in conventional homologous recombination, such as gene conversion with or without crossing over (Paques and Haber 1999; Sung *et al.* 2000). In our analysis, local gene conversion of the *URA3* marker was not observed in *rad51* mutants but the sample size was too small to fully evaluate the effect of the mutation (Tables 4 and 8). The frequency of allelic crossing over was decreased in *rad51* mutants only about twofold. The events we categorize as allelic crossing over could arise through reciprocal crossing over between homologous chromatids in the S-G_2 stages, as well as through a nonreciprocal BIR mechanism. When two DSBs on homologs are repaired by SSA involving allelic loci, the resulting chromosome would have the same structure as that produced by allelic crossing over as well. Because both BIR and SSA can occur in a *RAD51*-independent way, these notions explain why LOH events arising via allelic recombination were relatively common in *rad51* mutants. Allelic crossing-over events in the mutants, however, probably arise through different mechanisms from those in wild type.

A role for RAD50 in sister chromatid recombination: Among LOH events identified in *rad50* mutants, the frequencies of all types of recombination were increased >10-fold compared to those in Rad^+ cells, excluding the <2-fold increase in intrachromosomal deletion involving the *MAT-HMR* loci. Most events were *RAD52*-dependent, as seen by the large decrease in their frequency in *rad50 rad52* double mutants (Table 3 and Figure 2). This "hyper-recombination" phenotype of *rad50* mutants was also observed in previous studies of spontaneous interchromosomal recombination between heteroalleles (Malone *et al.* 1990). However, in this study, the most prominent LOH event in *rad50* mutants was chromosome loss, with a frequency comparable to that seen in other *rad* mutants. Taken together, we suggest that *RAD50* gene functions are required for chromosome maintenance by virtue of their role in sister chromatid recombination but that they are not always necessary for other types of recombination, especially recombination between different chromosomes. In the absence of sister chromatid recombination in *rad50* mutants, some lesions instead may be processed by available homologous recombination pathways, presumably those dependent on *RAD51* and/or on *RAD52*, thereby accounting for the observed increase of LOH events. A role of the MRX complex in sister chromatid recombination was previously proposed, on the basis of genetic analysis of X-ray-induced recombination (Ivanov *et al.* 1992; Bressan *et al.* 1998, 1999) and recent structural analysis of the *Pyrococcus furiosus* Rad50p and Mre11p (Hopfner *et al.* 2001; D'Amours and Jackson 2002). The role of Rad50p in sister chromatid recombination may also explain our observation that the increase in the frequency of intrachromosomal *MAT-HMR* deletion was much lower than that of other recombination events in *rad50* mutants. In this case, the deletion may have arisen primarily by recombination between sister chromatids rather than within the same chromosome molecule. Other types of recombination events detected in the LOH assay, in contrast, all involve interchromosomal interactions, which appear to be efficiently operated in the absence of *RAD50*. In addition

to its role in sister chromatid recombination, the MRX complex is also thought to resect the ends of DSBs, an initial step in DSB repair mediated by homologous recombination. In mutants deficient in the complex, the rate of 5′ to 3′ resection at HO-cut DSBs is reduced (Ivanov *et al.* 1994; Lee *et al.* 1998; Tsubouchi and Ogawa 1998). Our observation that spontaneous interchromosomal rearrangements can occur normally in the absence of Rad50p suggests that resection by the complex is not an absolute prerequisite or that lesions requiring resection are not a major source of rearrangements.

Alternative pathways of homologous recombination: The frequency of intragenic point mutation was increased to a similar extent in the *rad52* and *rad51* mutants, at least ~25-fold over that in Rad$^+$ cells. Such mutations were not observed for the *rad50* mutant, for which the possible maximum frequency is half the level of that of *rad52* and *rad51* mutants (Tables 4 and 8). The *rad52* mutation spectrum consisted of base substitution or −1 frameshifts, and in some clones two nearby mutations were found. These profiles are consistent with the postulated activity of an error-prone DNA polymerase that can mediate translesion DNA synthesis at a daughter strand gap across from a noncoding lesion. It has been reported that spontaneous and UV-induced mutations are increased by *rad51* or *rad52* mutations in haploids (Morrison and Hastings 1979; Roche *et al.* 1995; Liefshitz *et al.* 1998; Paulovich *et al.* 1998) and that *rad52*-provoked mutations of the *SUP4*-o gene are dependent on *REV3*, which encodes a catalytic subunit of an error-prone DNA polymerase in yeast (Roche *et al.* 1995), while the enhancement by the *rad* mutations in those studies was smaller than what we observed in this study. These results suggest that DNA lesions like daughter strand gaps are, at least in part, repaired primarily through *RAD52*- and *RAD51*-dependent recombination pathways and that in the absence of the primary pathways, some of these lesions are instead channeled to a second pathway that may be mutagenic, occasionally giving rise to point mutations. *RAD50* may contribute little to this daughter strand gap repair, since the MRX or Mre11-Rad50 complex is known to preferentially bind double-stranded DNA ends (Chen *et al.* 2001; De Jager *et al.* 2001; D'Amours and Jackson 2002). In addition, homologous recombination pathways other than those acting on sister chromatids are proficient in *rad50* mutants, as observed in this study, and they may repair daughter strand gaps prior to the intervention of an alternative mutagenic pathway. These proposals explain the observation that intragenic mutation was not induced by the *rad50* mutation, at least to the level of *rad51* and *rad52* mutants.

It is possible that DSB repair by NHEJ, another alternative pathway for homologous recombination, causes intragenic mutations because NHEJ often leaves small insertions or deletions at the junction of joining. Around the sites of frameshift mutations obtained in *rad52* mutants, however, there were no sequences >1 bp that would allow a misalignment to give rise to a frameshift through a NHEJ mechanism. Among the aberrant chromosomes identified in *rad52* mutants, there was a translocation with 4 bp of microhomology at the breakpoints that is likely to have arisen through a NHEJ mechanism. In the previous analysis of LOH in Rad$^+$ cells, we did not recover aberrant chromosomes with breakpoints indicative of NHEJ (Umezu *et al.* 2002). However, from these results we cannot conclude that NHEJ was induced in *rad52* mutants because in Rad$^+$ cells NHEJ could be masked by the more efficient homologous recombination.

In either case, the results obtained for *rad52* and *rad51* mutants clearly indicate that in the absence of the major homologous recombination pathways, mutagenic events are promoted by alternative pathways, most likely translesion DNA synthesis and NHEJ. These results do not exclude the possibilities that in some circumstances these alternative pathways function primarily prior to homologous recombination or act as precise repair mechanisms for certain DNA lesions. We are now investigating the roles of translesion DNA synthesis and NHEJ in genome maintenance by analyzing LOH events in cells defective for these pathways.

We are grateful to Tomoko Ogawa, Akira Shinohara, and Katsuhiko Shirahige for providing plasmids. We thank Jun Ajima and Satoshi Kawauchi for their comments on the manuscript. This work was supported by a Grant-in-Aid for Scientific Research on Priority Areas (B, 11239208 and 13141204 to K.U.; and C, 12213082 to H.M.) from the Ministry of Education, Culture, Sports, Science, and Technology.

LITERATURE CITED

Adzuma, K., T. Ogawa and H. Ogawa, 1984 Primary structure of the *RAD52* gene in *Saccharomyces cerevisiae*. Mol. Cell. Biol. **4:** 2735–2744.

Ajima, J., K. Umezu and H. Maki, 2002 Elevated incidence of loss of heterozygosity (LOH) in an *sgs1* mutant of *Saccharomyces cerevisiae*: roles of yeast RecQ helicase in suppression of aneuploidy, interchromosomal rearrangement, and the simultaneous incidence of both events during mitotic growth. Mutat. Res. **504:** 157–172.

Alani, E., L. Cao and N. Kleckner, 1987 A method for gene disruption that allows repeated use of *URA3* selection in the construction of multiply disrupted yeast strains. Genetics **116:** 541–545.

Alani, E., S. Subbiah and N. Kleckner, 1989 The yeast *RAD50* gene encodes a predicted 153-kD protein containing a purine nucleotide-binding domain and two large heptad-repeat regions. Genetics **122:** 47–57.

Astrom, S. U., S. M. Okamura and J. Rine, 1999 Yeast cell-type regulation of DNA repair. Nature **397:** 310.

Bai, Y., and L. S. Symington, 1996 A Rad52 homolog is required for *RAD51*-independent mitotic recombination in *Saccharomyces cerevisiae*. Genes Dev. **10:** 2025–2037.

Bennett, C. B., L. K. Lewis, G. Karthikeyan, K. S. Lobachev, Y. H. Jin *et al.*, 2001 Genes required for ionizing radiation resistance in yeast. Nat. Genet. **29:** 426–434.

Boulton, S. J., and S. P. Jackson, 1998 Components of the Ku-dependent non-homologous end-joining pathway are involved in telomeric length maintenance and telomeric silencing. EMBO J. **17:** 1819–1828.

Bressan, D. A., H. A. Olivares, B. E. Nelms and J. H. Petrini, 1998 Alteration of N-terminal phosphoesterase signature motifs inactivates *Saccharomyces cerevisiae* Mre11. Genetics **150:** 591–600.

Bressan, D. A., B. K. Baxter and J. H. Petrini, 1999 The Mre11-

Rad50-Xrs2 protein complex facilitates homologous recombination-based double-strand break repair in *Saccharomyces cerevisiae*. Mol. Cell. Biol. **19:** 7681–7687.

Chen, L., K. Trujillo, W. Ramos, P. Sung and A. E. Tomkinson, 2001 Promotion of Dnl4-catalyzed DNA end-joining by the Rad50/Mre11/Xrs2 and Hdf1/Hdf2 complexes. Mol. Cell **8:** 1105–1115.

Cox, M. M., M. F. Goodman, K. N. Kreuzer, D. J. Sherratt, S. J. Sandler *et al.*, 2000 The importance of repairing stalled replication forks. Nature **404:** 37–41.

D'Amours, D., and S. P. Jackson, 2002 The Mre11 complex: at the crossroads of DNA repair and checkpoint signalling. Nat. Rev. Mol. Cell. Biol. **3:** 317–327.

De Antoni, A., and D. Gallwitz, 2000 A novel multi-purpose cassette for repeated integrative epitope tagging of genes in *Saccharomyces cerevisiae*. Gene **246:** 179–185.

De Jager, M., J. van Noort, D. C. van Gent, C. Dekker, R. Kanaar *et al.*, 2001 Human Rad50/Mre11 is a flexible complex that can tether DNA ends. Mol. Cell **8:** 1129–1135.

Galgoczy, D. J., and D. P. Toczyski, 2001 Checkpoint adaptation precedes spontaneous and damage-induced genomic instability in yeast. Mol. Cell. Biol. **21:** 1710–1718.

Grenon, M., C. Gilbert and N. F. Lowndes, 2001 Checkpoint activation in response to double-strand breaks requires the Mre11/Rad50/Xrs2 complex. Nat. Cell Biol. **3:** 844–847.

Haber, J. E., 1999 DNA recombination: the replication connection. Trends Biochem. Sci. **24:** 271–275.

Heude, M., and F. Fabre, 1993 a/α-control of DNA repair in the yeast *Saccharomyces cerevisiae*: genetic and physiological aspects. Genetics **133:** 489–498.

Hiraoka, M., K. Watanabe, K. Umezu and H. Maki, 2000 Spontaneous loss of heterozygosity in diploid *Saccharomyces cerevisiae* cells. Genetics **156:** 1531–1548.

Hopfner, K. P., A. Karcher, L. Craig, T. T. Woo, J. P. Carney *et al.*, 2001 Structural biochemistry and interaction architecture of the DNA double-strand break repair Mre11 nuclease and Rad50-ATPase. Cell **105:** 473–485.

Ivanov, E. L., V. G. Korolev and F. Fabre, 1992 *XRS2*, a DNA repair gene of *Saccharomyces cerevisiae*, is needed for meiotic recombination. Genetics **132:** 651–664.

Ivanov, E. L., N. Sugawara, C. I. White, F. Fabre and J. E. Haber, 1994 Mutations in *XRS2* and *RAD50* delay but do not prevent mating-type switching in *Saccharomyces cerevisiae*. Mol. Cell. Biol. **14:** 3414–3425.

Kadyk, L. C., and L. H. Hartwell, 1992 Sister chromatids are preferred over homologs as substrates for recombinational repair in *Saccharomyces cerevisiae*. Genetics **132:** 387–402.

Kadyk, L. C., and L. H. Hartwell, 1993 Replication-dependent sister chromatid recombination in *rad1* mutants of *Saccharomyces cerevisiae*. Genetics **133:** 469–487.

Kagawa, W., H. Kurumizaka, S. Ikawa, S. Yokoyama and T. Shibata, 2001 Homologous pairing promoted by the human Rad52 protein. J. Biol. Chem. **276:** 35201–35208.

Kironmai, K. M., and K. Muniyappa, 1997 Alteration of telomeric sequences and senescence caused by mutations in *RAD50* of *Saccharomyces cerevisiae*. Genes Cells **2:** 443–455.

Klein, H. L., 1995 Genetic control of intrachromosomal recombination. Bioessays **17:** 147–159.

Klein, H. L., 1997 RDH54, a *RAD54* homologue in *Saccharomyces cerevisiae*, is required for mitotic diploid-specific recombination and repair and for meiosis. Genetics **147:** 1533–1543.

Klein, H. L., 2001 Spontaneous chromosome loss in *Saccharomyces cerevisiae* is suppressed by DNA damage checkpoint functions. Genetics **159:** 1501–1509.

Kuzminov, A., 1999 Recombinational repair of DNA damage in *Escherichia coli* and bacteriophage λ. Microbiol. Mol. Biol. Rev. **63:** 751–813.

Lee, S. E., J. K. Moore, A. Holmes, K. Umezu, R. D. Kolodner *et al.*, 1998 *Saccharomyces* Ku70, Mre11/Rad50 and RPA proteins regulate adaptation to G2/M arrest after DNA damage. Cell **94:** 399–409.

Liefshitz, B., R. Steinlauf, A. Friedl, F. Eckardt-Schupp and M. Kupiec, 1998 Genetic interactions between mutants of the 'error-prone' repair group of *Saccharomyces cerevisiae* and their effect on recombination and mutagenesis. Mutat. Res. **407:** 135–145.

Malone, R. E., T. Ward, S. Lin and J. Waring, 1990 The RAD50 gene, a member of the double strand break repair epistasis group, is not required for spontaneous mitotic recombination in yeast. Curr. Genet. **18:** 111–116.

Morrison, D. P., and P. J. Hastings, 1979 Characterization of the mutator mutation *mut5–1*. Mol. Gen. Genet. **175:** 57–65.

Mortimer, R. K., R. Contopoulou and D. Schild, 1981 Mitotic chromosome loss in a radiation-sensitive strain of the yeast *Saccharomyces cerevisiae*. Proc. Natl. Acad. Sci. USA **78:** 5778–5782.

Nugent, C. I., G. Bosco, L. O. Ross, S. K. Evans, A. P. Salinger *et al.*, 1998 Telomere maintenance is dependent on activities required for end repair of double-strand breaks. Curr. Biol. **8:** 657–660.

Ogawa, T., A. Shinohara, A. Nabetani, T. Ikeya, X. Yu *et al.*, 1993 RecA-like recombination proteins in eukaryotes: functions and structures of *RAD51* genes. Cold Spring Harbor Symp. Quant. Biol. **58:** 567–576.

Paques, F., and J. E. Haber, 1999 Multiple pathways of recombination induced by double-strand breaks in *Saccharomyces cerevisiae*. Microbiol. Mol. Biol. Rev. **63:** 349–404.

Paulovich, A. G., C. D. Armour and L. H. Hartwell, 1998 The *Saccharomyces cerevisiae RAD9*, *RAD17*, *RAD24* and *MEC3* genes are required for tolerating irreparable, ultraviolet-induced DNA damage. Genetics **150:** 75–93.

Roche, H., R. D. Gietz and B. A. Kunz, 1995 Specificities of the *Saccharomyces cerevisiae rad6*, *rad18*, and *rad52* mutators exhibit different degrees of dependence on the *REV3* gene product, a putative nonessential DNA polymerase. Genetics **140:** 443–456.

Rose, M. D., F. Winston and P. Hieter, 1990 *Methods in Yeast Genetics: A Laboratory Course Manual*. Cold Spring Harbor Laboratory Press, Cold Spring Harbor, NY.

Sambrook, J., and D. W. Russell, 2001 *Molecular Cloning: A Laboratory Manual*, Ed. 3. Cold Spring Harbor Laboratory Press, Cold Spring Harbor, NY.

Sambrook, J., E. F. Fritsch and T. Maniatis, 1989 *Molecular Cloning: A Laboratory Manual*, Ed. 2. Cold Spring Harbor Laboratory Press, Cold Spring Harbor, NY.

Shibata, T., T. Nishinaka, T. Mikawa, H. Aihara, H. Kurumizaka *et al.*, 2001 Homologous genetic recombination as an intrinsic dynamic property of a DNA structure induced by RecA/Rad51-family proteins: a possible advantage of DNA over RNA as genomic material. Proc. Natl. Acad. Sci. USA **98:** 8425–8432.

Shinohara, A., H. Ogawa and T. Ogawa, 1992 Rad51 protein involved in repair and recombination in S. cerevisiae is a RecA-like protein. Cell **69:** 457–470.

Signon, L., A. Malkova, M. L. Naylor, H. Klein and J. E. Haber, 2001 Genetic requirements for *RAD51*- and *RAD54*-independent break-induced replication repair of a chromosomal double-strand break. Mol. Cell. Biol. **21:** 2048–2056.

Sung, P., K. M. Trujillo and S. Van Komen, 2000 Recombination factors of *Saccharomyces cerevisiae*. Mutat. Res. **451:** 257–275.

Tsubouchi, H., and H. Ogawa, 1998 A novel *mre11* mutation impairs processing of double-strand breaks of DNA during both mitosis and meiosis. Mol. Cell. Biol. **18:** 260–268.

Umezu, K., M. Hiraoka, M. Mori and H. Maki, 2002 Structural analysis of aberrant chromosomes that occur spontaneously in diploid *Saccharomyces cerevisiae*: retrotransposon Ty1 plays a crucial role in chromosomal rearrangements. Genetics **160:** 97–110.

Usui, T., H. Ogawa and J. H. Petrini, 2001 A DNA damage response pathway controlled by Tel1 and the Mre11 complex. Mol. Cell **7:** 1255–1266.

Watanabe, K., J. Morishita, K. Umezu, K. Shirahige and H. Maki, 2002 Involvement of *RAD9*-dependent damage checkpoint control in arrest of cell cycle, induction of cell death, and chromosome instability caused by defects in origin recognition complex in *Saccharomyces cerevisiae*. Eukaryot. Cell **1:** 200–212.

Communicating editor: L. S. Symington